

DOI: 10.24425/amm.2019.130112

G. STRADOMSKI<sup>#</sup>, M. NADOLSKI\*, A. ZYSKA\*, B. KANIA\*\*, D. RYDZ\*

### PHYSICAL AND NUMERICAL MODELING OF DUPLEX CAST STEEL THIN-WALLED CASTINGS

The paper, which is a summary and supplement of previous works and research, presents the results of numerical and physical modeling of the GX2CrNiMoCuN25-6-3 duplex cast steel thin-walled castings production. To obtain thin-walled castings with wall in the thinnest place even below 1 mm was used the centrifugal casting technology and gravity casting. The analyzed technology (centrifugal casting) enables making elements with high surface quality with reduced consumption of batch materials and, as a result, reducing the costs of making a unitary casting. The idea behind the production of cast steel with the use of centrifugal technology was to find a remedy for the problems associated with unsatisfactory castability of the tested alloy.

The technological evaluation of the cast construction was carried out using the Nova Flow & Solid CV 4.3r8 software. Numerical simulations of crystallization and cooling were carried out for a casting without a gating system and sinkhead located in a mold in accordance with the pouring position. It was assumed that the analyzed cast will be made in the sand form with dimensions 250×250×120 mm.

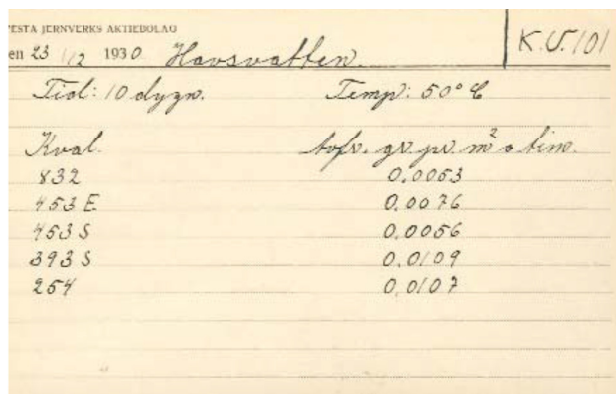
*Keywords:* duplex cast steel, centrifugal casting, gravity casting, thin-walled castings

#### 1. Introduction

Materials which, for more than 40 years, regardless of prosperity or crises periods, constantly have about 5% annual increase in production are corrosion resistant steels and cast steels. Very highly diverse of properties, depending on the chemical composition and microstructure constantly expand areas of applications of these materials. A special group between those materials are ferritic-austenitic steels whose development allows to increase the durability of elements exposed to erosion and corrosion wear or exploitation of deeply depleted, strongly sulphated gas and oil deposits. The origin and development of

duplex steels are associated with the appearance of corrosion resistant steels in the early of the 20th century [1-7].

According to Olsson and Sinis [8], the first attempts with this type of materials were made at the Avesta research center on December 23, 1930. However, these grades were not designed as engineering material because the metallurgical processes in those years did not allow to obtain the correct content of ferrite and austenite, and the addition of nitrogen was almost impossible. That limited the production of material for cast and forged products (Fig. 1). Significant acceleration of work on duplex steels occurred after World War II and was caused by a nickel deficit in global markets [6-10].



Kval.	Wsp. gę. gę. m <sup>2</sup> s <sup>2</sup> km.
832	0,0053
453E	0,0076
453S	0,0056
393S	0,0109
257	0,0102



Fig. 1. Protocol from 1930 describing the study of duplex stainless steel grade 453S with 25% Cr, 1.5% Mo (left side), gunpowder reactor of the same steel grade supplied to a Belgian factory in 1933 (right side) [11]

\* CZESTOCHOWA UNIVERSITY OF TECHNOLOGY, FACULTY OF PRODUCTION ENGINEERING AND MATERIALS, 19 ARMII KRAJOWEJ AV., 42-200 CZĘSTOCHOWA, POLAND

\*\* INSTITUTE OF METALLURGY AND MATERIALS SCIENCE OF POLISH ACADEMY OF SCIENCES, 25 W. REYMONTA STR., 30-059 KRAKÓW, POLAND

# Corresponding author: stradomski.grzegorz@wip.pcz.pl

The basic application area of ferritic-austenitic steels and cast-steels, also called duplexes, are constructions and elements exposed to high loads and environments conducive to the formation of stress, pitting or crevice corrosion. In such conditions, ferritic-austenitic steels and cast-steels with a comparable share of basic phases - ferrite and austenite, show a better set of mechanical properties compared to traditional ferritic or austenitic steels. Higher than in the case of austenitic cast steels, mechanical properties and good resistance to general and pitting corrosion cause that duplex steels and cast-steels have become today irreplaceable for example in food industry, the chemical industry, in the construction of warehouses and tanks for ships transporting products with high chemical activity – acid phosphoric, concentrated sulfuric acid, strongly alkaline media or devices used in the petrochemical, energy, pulp and paper industry [9-14].

The centrifugal casting technology is most often used for producing castings in the form of bodies of revolution without core-making. The mold is set in rotating motion around the vertical, horizontal and inclined axes. It is also able to rotate simultaneously around mutually perpendicular axes, e.g. the vertical and horizontal ones [15-17]. Shape castings, on the other hand, are made in a mold or molds arranged on the edges of the disc of the centrifugal pourer with a vertical axis of rotation. According to literature data [18] centrifugal casting technology give possibility to obtain products with a mass from several grams (micro casting) to several tones, whereas thin-walled casts with a diameter of up to 700 mm with a maximum weight of around 1 tons are made for machines with a horizontal axis of rotation. Golowin gives an example of a 45-ton cast of a centrifugally cast ingot with a vertical axis of rotation [15].

## 2. Material and methodology of research

Due to the difficulty of utilizing the corrosion resistant steel scrap with copper, an additional requirement was assessed. The possibility of eliminating Cu - an element that strongly increases castability. For the tests the GX2CrNiMoN25-6-3 cast steel was selected (Table 1).

TABLE 1

Chemical composition of the GX2CrNiMoN25-6-3 cast steel [% mass.]

C	Mn	Si	S	P	Cr	Ni	Mo	Cu	N
0.021	1.46	0.93	0.012	0.008	26.70	6.48	3.10	0.02	0.23

The conducted research was divided into the following stages:

- Prediction of cast shape, radial pump with a diameter of 180 mm and blade thickness from about 5 to 1 mm,
- Numerical simulations of the crystallization and cooling process based on for the Nova Flow & Solid CV 4.3r8 software,
- Comparison of obtained centrifugal castings with a cast made in the gravitational technology,

- Evaluation of the obtained casts microstructure and heat treatment,
- Tests of the state of internal stresses carried out by the  $\sin^2\psi$  method.

For the tests was selected produced in the country, a small-sized radial pump rotor used for highly saline and sandy water. This element (Fig. 2) has been so far made mainly of non-ferrous alloys. Use of duplex cast-steel for such element would be a valuable complement to the production offer due to its mechanical and functional properties. In the analyzed casting, the minimum blade thickness is about 1 mm, which is a technological challenge and was an incentive to undertake this research.

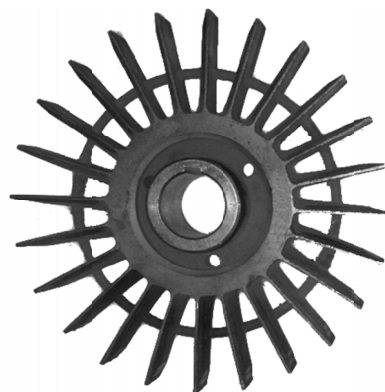


Fig. 2. The selected shape of the cast used in the research

The idea behind the production of cast steel with the use of centrifugal technology was to find a remedy for related problems with unsatisfactory castability of the alloy. The tested cast steel due to the chemical composition – low content of carbon, high chromium over 21%, nickel about 6%, and the addition of such elements as molybdenum or nitrogen, is characterized by reduced casting properties. While in the case of castings with a considerable wall thickness, this is not a significant problem, whereas



Fig. 3. A view of an exemplary gravity cast with marked massive sinkhead

in the case of thin-walled castings it is an important obstacle [14,19-21]. The main disadvantages occurring in thin-walled castings are the incorrect mapping of the mold and the disadvantages of the shrink type. An effective solution to these problems may be to increase the casting module over the recommended 30%, or to trigger the appropriate metallostatic pressure inside the mold. The use of an increased sinkhead is characterized by a very significant, reaching up to 2/3 of the weight of the finished casting, waste, figure 3.

### 3. Results

As it was already mentioned in the research, authors made a task to make thin-walled castings from a copper-free alloy. The second assumption was to reduce the amount of obtained scrap. For this purpose, the use of centrifugal casting has been proposed, thanks to which it is possible to force the directional flow of metal in the mold, thus mapping even thin walls is

possible. Based on the selected industrial cast (Fig. 2), a CAD model was developed and next a model of rotor was made by 3D printing, as shown in Figure 4.

The assessment of the manufacturability of the casting structure was accomplished using the NovaFlow&Solid CV 4.3r8 program. Numerical simulations of cooling and solidifying processes were performed for the casting without a gating system or sinkheads, placed in the mold according to the desired pouring position. It was assumed that the analyzed casting would be produced in the sand mold of dimensions equal to 250×250×120 mm. The purpose of calculation was to identify the primary thermal centers within the casting and to find the shrinkage porosity distribution after the complete solidification. The thermal problem was solved with omission of the mold pouring and filling stages. It was assumed that at the initial moment the mold is 100% filled with liquid metal, and the initial temperature in every point of the melt is equal to 1600°C.

Bright fields on the temperature map and map of the liquid phase represented by local heat centers in the cast, whose

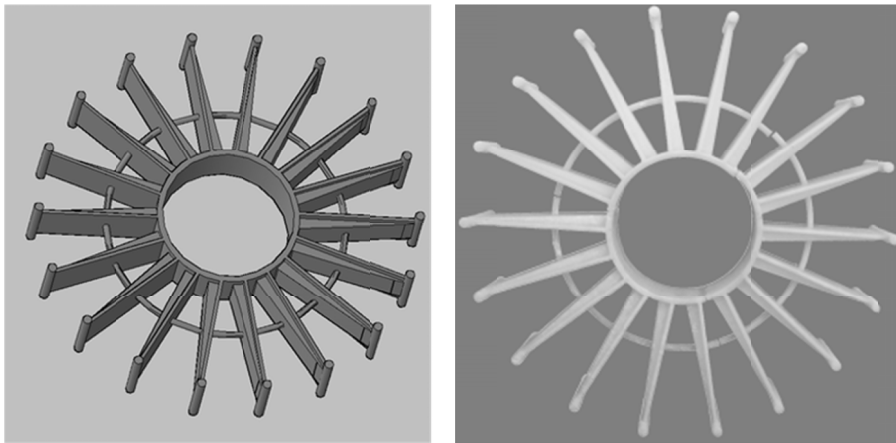


Fig. 4. View of the CAD model and 3D printout of the rotor model

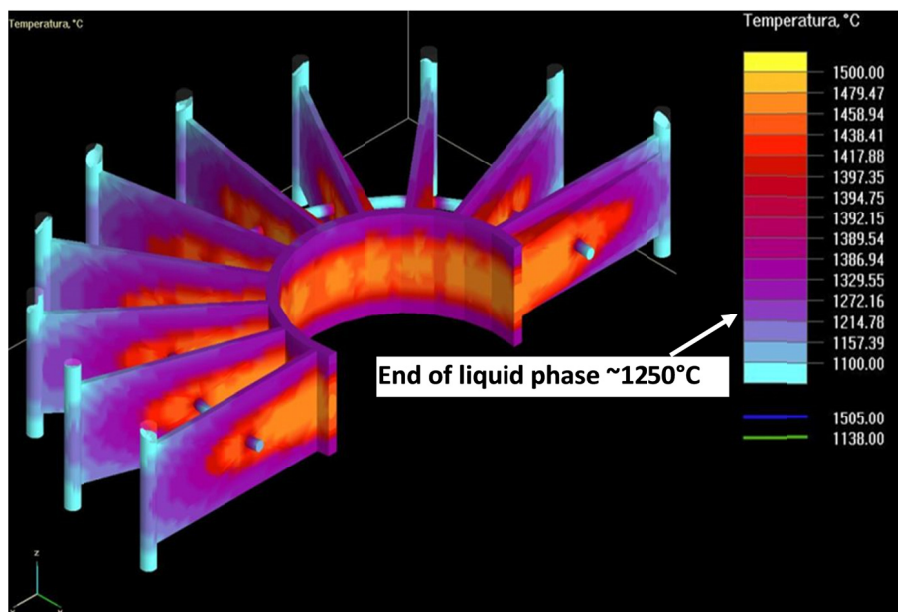


Fig. 5. Momentary temperature field in the final stage of solidification

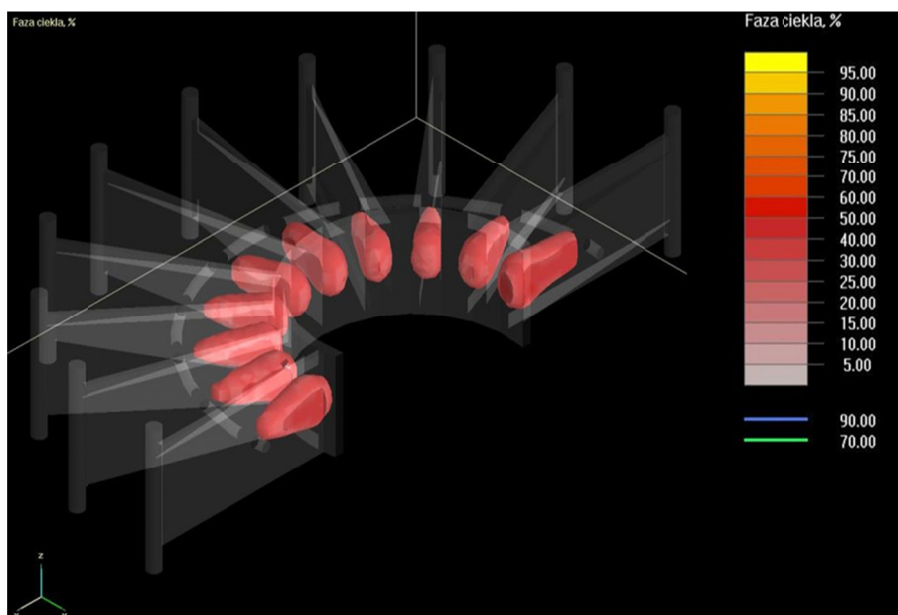


Fig. 6. Distribution of the residual liquid within the casting in the final stage of solidification (10% of liquid phase)

presence results in high probability of occurrence of shrinkage defects. It was assumed that the presence of the liquid phase in the final stage of the simulated solidification. The presence of liquid phase (Fig. 6) should contribute to the better feeding of the casting, finally eliminating its slight porosity.

In the next step, a series of thin-walled castings were made using two techniques, ie gravity and centrifugal casting. On the basis of the 3D print, thin-walled ceramic mold were made according to the investment pattern technology in the solution with a support layer. So prepared mold, after the pattern fusing and baking process, was cooled down to a temperature of about 500°C-550°C. At this temperature, the mold was mounted on the vertical rotation axis centrifugal pouring stand. To establish the preliminary pouring process parameters, three series of castings were made with basic process parameters, as shown in Table 2.

In the case of the S1 casting, the poured mold was put into spine movement in the shortest possible time. In the case of

TABLE 2

The applied parameters of the casting process

Designation	Pouring temperature [°C]	Form movement during casting / Rotation speed [rpm]/ casting time [s]
S1	1550	Stationary /200/~2
S2	1550	Spinning /250/~2
S3	1550	Stationary /0/~1.5
S4	1650	Stationary /0/~2

a rotating mold, the alloy was introduced during the spinning of the mold after reaching the steady state. The spinning time of the castings during the crystallization was 2 min, and after about 5 min the casting was stamped out of form for the purpose of free crystallization. The element marked as S4 is a gravity cast using an increased sinkhead and comes from technological trials made in the classic molding mass in a block form. Figure 7 shows the appearance of castings S1 and S4.

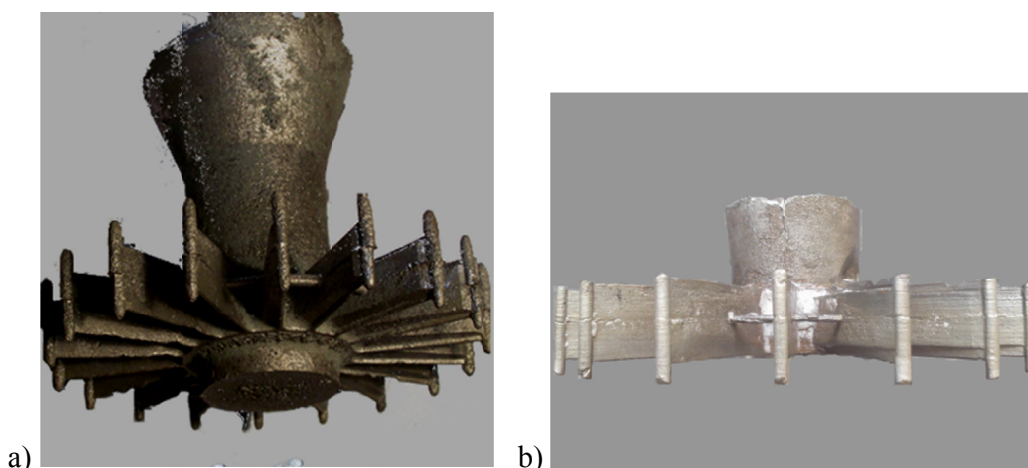


Fig. 7. View of the rotor: a) made in gravity technology S4 and b) centrifugal cast

As it can be seen the complex shape and surface quality of thin-walled gravity castings, was managed to reproduce satisfactorily as the centrifugal ones in a very good way. Very low surface roughness of the blades in the case of the proposed centrifugal technology greatly limits machining. The obtained casting surface roughness results are summarized in Table 3.

TABLE 3

Surface roughness results

Series	1	2	3	4
$R_a$ $\mu\text{m}$	4.65	4.39	7.34	12.79
$R_z$ $\mu\text{m}$	19.1	20.0	40.9	59.2

In a further stage of the tests, the microstructure of the casting's working parts, ie the rotor blades, was assessed. The analysis was carried out in three areas end, center and axis. The microstructure in all three research areas of the blade was similar, therefore in the next part it will be presented only from the middle part. Samples were etched with the Mi21Fe reagent, and Figure 8 shows the microstructure.

The analysis of the microstructure S1, S2 and S4 indicates a strong similarity both in terms of grain size and the share of individual structural components, whose share determined by percentage of ferrite content was about 54, 58 and 49%. The phase share was determined using the Nis-Elements D software.

Strictly determined crystallization and cooling rates of a thin-walled rotor casting, associated with the cast construc-

tion, the type of materials used and the thickness of the mold enable obtaining a fine (dendritic) ferritic-austenitic structure and about 10% of the  $\sigma$  phase (S4). This phase ( $\text{Fe}_{52}\text{Cr}_{48}$ ) according to many literature data has a hexagonal crystallographic structure characterized by high hardness and packing, generates very high compressive stresses [9,11,13,14,18,21-24]. In spite of its considerable participation, this quantity should result in an increase in brittleness and cracking of the castings (Fig. 9a), the material is characterized by exceptional plasticity (Fig. 9b) [22].

An important and interesting problem observed during researches was the explanation of the phenomenon of high plasticity of the cast-steel (S4) in spite of a significant amount of the  $\sigma$  phase. According to literature data [23,24] and own research, the reason for castings cracking already at the content exceeding 5% of the  $\sigma$  phase is the state of internal stresses generated by this phase reaching up to various sources of 2-3.5GPa.

In this work, the stress state was tested using the method  $\sin^2\psi$  using an X-ray diffractometer Bruker D8 Discover with polycapillary primary beam optics, 1.0 mm pinhole collimator and positional sensitive LynxEye semiconductor detector with 2.6 degree scale  $2\theta$  [25-27]. In the stress measurements, on the secondary beam side, a Soller collimator with angular divergence of 0.34 degrees was used (parallel beam configuration, enabling precise determination of the diffraction peak position for each angle value  $\psi$ ). For the research was used filtered radiation  $\text{CoK}\alpha$ . The sample was positioned in the apparatus using the Euler wheel and the X-Y-Z table. From the point of view of the geometry of stress measurement, the diffractometer worked in

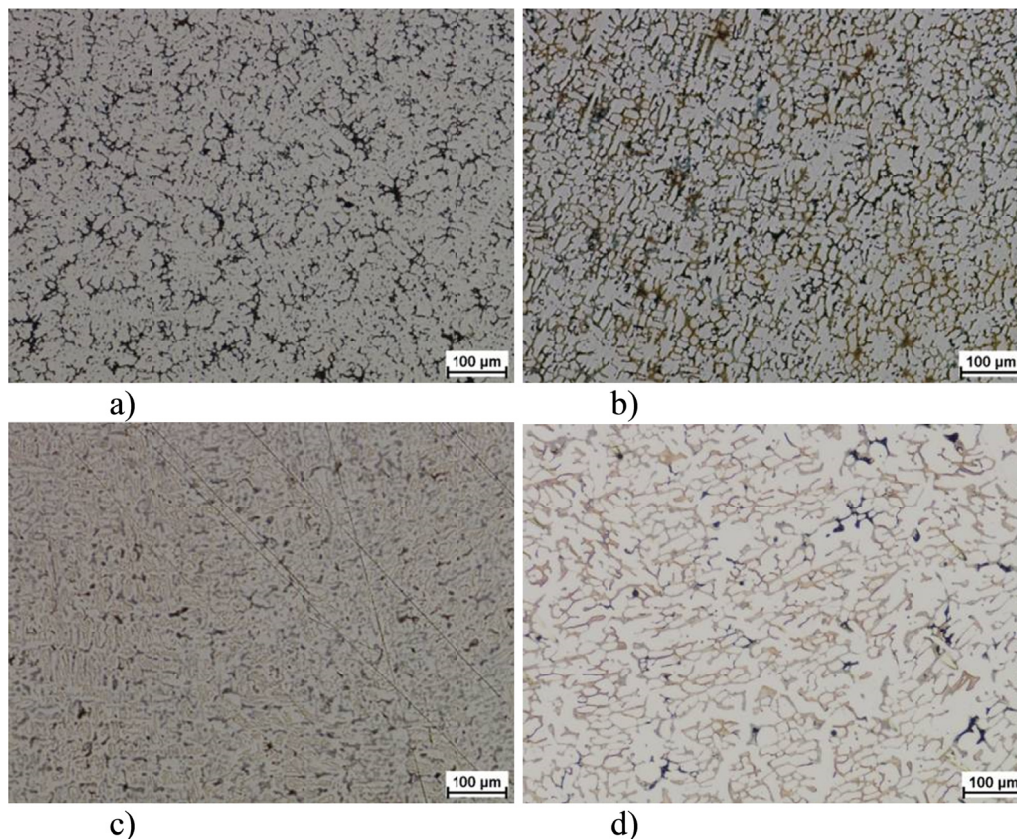


Fig. 8. Microstructure of the tested cast steel in the raw condition 100 $\times$ , a) S1, b) S2, c) S3, d) S4 – light microscope



Fig. 9. View of thin-wall blades made by various techniques

the system  $\psi$ . The control and analytical software – TARSiUS package [25-27] was used in the research. The analysis confirmed the results of measurements taken assumption:  $\sigma_{33} = \sigma_{13} = \sigma_{23} = 0$ . The directional stress measurement used to calculate the main stress system was made using the classic technique  $\sin^2\psi$  for four angle values  $\varphi$  on the surface of the sample. The range of angles used  $\psi$  was in the range  $\psi = 0^\circ$  to  $\psi = 65^\circ$  with a step  $\Delta\psi = 5^\circ$ . In each measurement a different range of angles was applied, depending on the position of the peak, its half width, intensity and planned measurement task (shorter / longer stress measurement) using a fixed step on the scale  $2\theta$ ;  $\Delta 2\theta = 0.02^\circ$ . The estimation of the uncertainty of the final results was based on the total differential method and the results of directional stress measurements, where the uncertainty was related to the quality of the linear model fit to the observed changes in the diffraction reflection positions.

Figure 10b shows the examined blade and the structure revealed by electropolishing (Fig. 10a) and the microstructure etched with the Mi21Fe reagent (Fig. 10c).

The obtained values of angular positions of diffraction reflection, were converted into network deformations, and then using X-ray solids of elasticity of single crystals  $E_{\alpha\text{-Fe.101}} = 233$  GPa,  $\nu_{\alpha\text{-Fe.101}} = 0.275$ ,  $E_{\gamma\text{-Fe.111}} = 300$  GPa,  $\nu_{\gamma\text{-Fe.111}} = 0.183$ , the level of own stresses, whose values are shown in table 4, was determined.

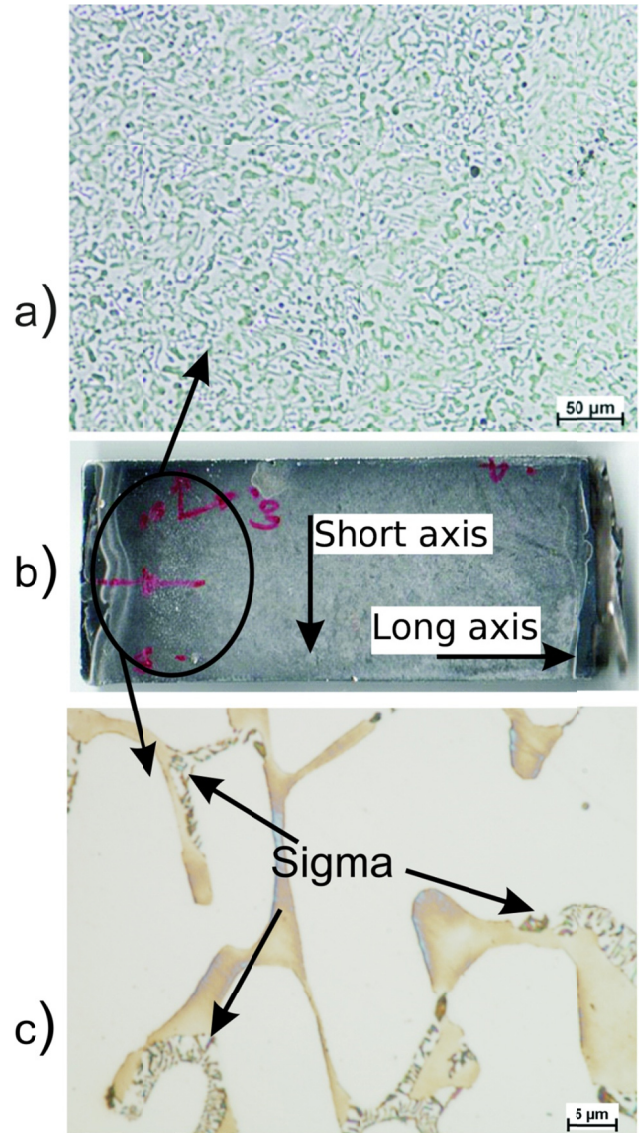


Fig. 10. The appearance of the rotor blade subjected to the XRD test a), electrolytic polishing b), etched with the Mi21Fe reagent magn. 1000 $\times$  c)

TABLE 4

Results of stress measurement in a thin-walled blade with gravity and centrifugal casting

Gravity casting S4	
Direction of measurement	$\sigma_\varphi$ [MPa]
<b>Ferrite</b>	
Shorter blade axis	$-550 \pm 100$
Longer blade axis	$-150 \pm 40$
<b>Austenite</b>	
Shorter blade axis	$-700 \pm 60$
Longer blade axis	$-450 \pm 80$
Centrifugal casting S1	
Direction of measurement	$\sigma_\varphi$ [MPa]
<b>Ferrite</b>	
Shorter blade axis	$-1175 \pm 60$
Longer blade axis	$-780 \pm 40$
<b>Austenite</b>	
Shorter blade axis	$-870 \pm 60$
Longer blade axis	$-550 \pm 80$

Results of stress measurement obtained with the  $\sin^2\psi$  method presented in table 4 indicate the presence of very high compressive stresses both in the austenite and in ferrite caused by very high stresses generated by the  $\sigma$  phase [23,24]. Measured values of compressive stresses, in the gravity casting S4, should guarantee obtaining higher plastic properties, which is observed. In the case of centrifugal casting, the stress values are much higher which is visible in its greater tendency to cracking. In the microstructure of blades, were observed fine precipitation of the  $\sigma$  phase uniformly distributed in the entire volume, additionally in the S1 and S2 castings, a visible directionality of the grain orientation associated with the rotational movement was observed. As previous work [14,28,29] indicates, such a distribution of the  $\sigma$  phase increases the plastic properties and erosive resistance of the ferritic-austenitic cast steel. It should be noted, however, that this effect is obtained by a rather long and specific method of casting cooling, while the centrifugal casting from pouring into the mold to breaking out of form the time was 7 minutes, and further cooling took place in the open air. A quick transition through the range 900-600°C should protect against the precipitation of the  $\sigma$  phase, in this case, it did not succeed and the amount of the  $\sigma$  phase was significant about 10%. Interestingly, despite the similar nature of the precipitations, the effect of high plasticity on cold that was observed in the case of the gravity casting S4 was not achieved. Centrifugal castings, especially S2, were characterized by lower plasticity. In order to eliminate this phenomenon, heat treatment of S1-S3 castings was carried out according to the recommendations presented in table 5.

TABLE 5

Parameters of the applied heat treatment

Treatment	S1	S2	S3
Supersaturation 1	1050°C for 90 min		
Supersaturation 2	1100°C for 120 min		
Supersaturation 3	1100°C for 240 min		

Figure 11 present the microstructure of castings after supersaturation according to table 5.

The microstructure of S1 and S2 castings after the applied heat treatment is very similar. Literature data [10,11,21], including those concerning steel and duplex cast steels, determine that the correct content of ferrite and austenite should be close to 50%. Deviations from these values are permissible, however, from the point of view of corrosion resistance, this share should not be lower than 30 to 70% (ferrite / austenite) [30]. Table 6 shows the obtained values of the ferrite fraction after the applied treatments.

TABLE 6

Measured values of the ferrite fraction after the applied treatments obtained with use of the Nis-Elements D

Designation	The share of ferrite [%]			
	Raw state	Supersaturation 1	Supersaturation 2	Supersaturation 3
S1	54%	53%	50%	55%
S2	58%	56%	55%	53%
S3	36%	47%	52%	54%

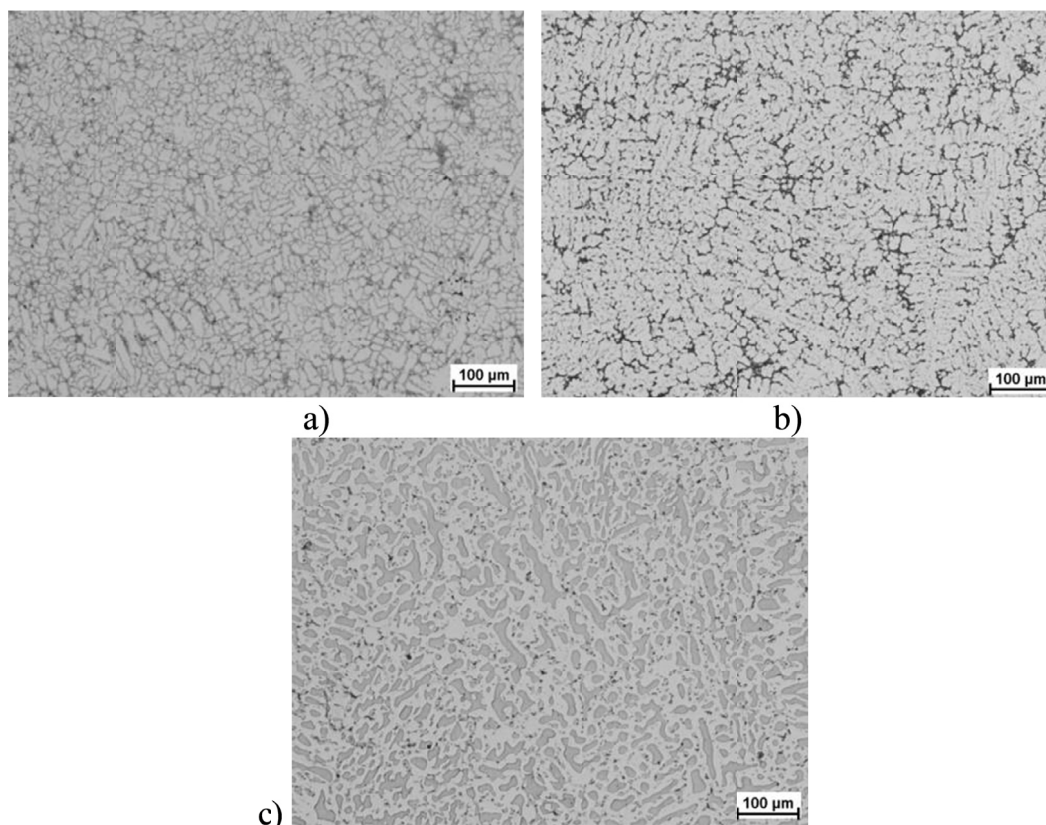


Fig. 11. Microstructure of tested castings after supersaturation 3; a) S1, b) S2, c) S3 – magn. 100×

#### 4. Conclusion

The presence of large  $\sigma$  phase precipitations are harmful due to a reduction of both corrosion resistance and plastic properties of duplex steel. Therefore, elements subjected to strong interaction of dynamic loads working in aggressive environments should have a very special kind of those precipitations, most preferably in the form of very fine inside grains of ferrite. They are totally unacceptable any precipitations on the grain boundaries, and in particular in the form of large aggregates. Therefore, after the detection, in the raw state, of  $\sigma$ -phase precipitates on the boundaries of ferrite and austenite grains, and high-direction microstructure, supersaturation processes were carried out. In the raw state, S1 and S2 castings were characterized by a similar microstructure and morphology and number of  $\sigma$  phase precipitates. After supersaturation from 1050°C and 90 minutes, the  $\sigma$  phase was not completely eliminated. For S1 castings, the sufficient supersaturation time was 120 minutes at 1100°C, while for S2 and S3 the necessary time was 240 minutes. Well observed directionality of the microstructure even after supersaturation is maintained. Obtaining fine, directed grains should guarantee high mechanical and functional properties. The use of centrifugal casting has a significant impact on increasing the surface quality of finished castings and reduces the amount of scrap generated. The proposed technology allows to eliminate the addition of copper increasing the castability of the tested alloy.

#### REFERENCES

- [1] C. Shargay, *Stainless Steel World* **17**, 19-27, (2005).
- [2] L. Marken, Application of duplex and super duplex stainless steels in the offshore industry- Case histories. *Stainless Steel World Conference & Expo*, 318-323, (2005).
- [3] T. Cassagne, F. Busschaert, Experience with duplex stainless steels in oil and gas production, *Duplex 2007 Conference*, *Stainless Steel World* (2007).
- [4] M. Dupouiron, F. Verneau, J.P. Audouard, J. Charles, Industrial experience of duplex and superduplex stainless steel in the chemical, mineral and petrochemical industries, 4th International Conference "Duplex Stainless Steel", 2-14 (1994).
- [5] K. Forch, Ch. Gillessen, I. von Hagen, *Stahl u. Eisen* **112** (4), 53-62 (1992).
- [6] J. Charles, *Revue de Métallurgie* **105** (03), 155-171 (2008).
- [7] <http://timesmachine.nytimes.com/timesmachine/1915/01/31/301779222.html#> accessed: 01.10.2015.
- [8] J. Olsson, M. Sinis, *Science Direct Desalination* **205**, 104-113 (2007).
- [9] Z. Stradomski, M.S. Soiński, G. Stradomski, *Archives of Foundry Engineering* **10** (2), 159-162 (2010).
- [10] J. Nowacki, *Stal dupleks w konstrukcjach spawanych*. Wydawnictwo Naukowo-Techniczne 2013, Warszawa (2013).
- [11] *Practical Guidelines for Fabrication of Duplex Stainless Steels*. International Molybdenum Association (2009).
- [12] D. Dyja, Z. Stradomski, C. Kolan, G. Stradomski, *Thermec 2012. Materials Science Forum* **706-709**, 2314-2319 (2012).
- [13] G. Stradomski, M.S. Soiński, K. Nowak, A. Szarek, *Steel Research International Spec. Edition Metal Forming 1231-1234* (2012).
- [14] G. Stradomski, *Oddziaływanie morfologii fazy sigma na kształtowanie właściwości stali i staliwa duplex*, Seria Monografie Częstochowa (2016).
- [15] S.J. Gołowin, *Special casting methods*, WNT Warszawa (1963).
- [16] Z. Górny, *Cast in rotating molds*, WNT Warszawa (1966).
- [17] W.S. Ebhotaa, A.S. Karunb, F.L. Inambao, *International Journal of Materials Research* **107**, 1-10 (2016).
- [18] *Collective Work: Engineer's Guide – Casting*, WNT Warszawa 1972.
- [19] D. Dyja, Z. Stradomski, *Archives of Foundry* **6** (19), 81-88 (2006).
- [20] G. Stradomski, *Archives of Foundry Engineering* **14** (3), 83-86 (2014).
- [21] Z. Stradomski, *The microstructure in problems of wear-resistant steel castings*, Technical University of Czestochowa (2010).
- [22] G. Stradomski, *Hutnik Wiadomości Hutnicze* **1**, 122-125 (2015).
- [23] R. Dos Santos, H.G. Priesmeyer, P.R. Sahn, *Giessereiforschung* **54** (2), 45-55 (2002).
- [24] H. von Eckhart, R. Dos Santos, *Giesserei* **91** (01), 18-28 (2004).
- [25] B. Kania, *Texture-Aided Residual Stress Identification System (TARSIS)*, in: *Sprawozdanie roczne 2014*, IMIM PAN, Kraków (2014).
- [26] B. Kania, P. Indyka, L. Tarkowski, E. Bełtowska-Lehman, *Journal of Applied Crystallography* **8**, 71-78 (2015).
- [27] J.T. Bonarski, B. Kania, K. Bolanowski, A. Karolczuk, *Archives of Metallurgy and Materials* **3** (60), 2247-2252 (2015).
- [28] G. Stradomski, M. Nadolski, Z. Stradomski, *Archives of Foundry Engineering* **15** (3), 57-60 (2015).
- [29] G. Stradomski, M. Nadolski, Z. Stradomski, *Archives of Foundry Engineering* **15** (3), 77-82 (2015).
- [30] L. Ping, C. Qizhou, W. Bokang, *Engineering Failure Analysis* **13**, 876-885 (2006), DOI: 10.1016/j.engfailanal.2005.07.004.